ISTITUTO NAZIONALE DI FISICA NUCLEARE

Sezione di Genova

INFN/AE–98/17
6 Luglio 1998

A. Petrolini:

RECENT PHYSICS RESULTS WITH THE RING IMAGING CHERENKOV DETECTOR OF THE DELPHI EXPERIMENT AT LEP

Expanded version of a talk presented at the "1998 Joint AAPT/APS Meeting", April 18–21, 1998, Columbus, OH

Published by ***SIS–Pubblicazioni***
Laboratori Nazionali di Frascati

INFN – Istituto Nazionale di Fisica Nucleare
Sezione di Genova

INFN/AE–98/17
6 Luglio 1998

Recent physics results with the Ring Imaging Cherenkov detector of the DELPHI experiment at LEP

Alessandro Petrolini

Dipartimento di Fisica dell'Università di Genova and INFN

Via Dodecaneso 33, I-16146 Genova, Italy

E-mail: petrolini@genova.infn.it

Abstract

A brief overview is presented of some recent physics results obtained by the DELPHI experiment at LEP using the charged particle identification capability provided by its Ring Imaging Cherenkov detector.

1 Introduction

A brief overview is presented of some recent physics results obtained by the DELPHI experiment at LEP using the charged particle identification capability provided by its Ring Imaging Cherenkov (RICH) detector. A selection among the various topics had to be done necessarily done. Emphasis is given to the basic ideas while for technical details the reader is referred to the bibliography.

2 Particle identification with the DELPHI detector at LEP

The DELPHI experiment[1] at the Large Electron-Positron collider (LEP) at CERN is equipped with a Ring Imaging Cherenkov detector to perform charged particle identification.[2] Particle identification is a fundamental tool in high energy physics experiments and different methods are available according to the identity and energy of the particles one wishes to identify.

The specific energy loss by ionization depends on the particle mass and velocity and can therefore be used to identify particles. The information from the electromagnetic and hadronic calorimeters can also be used to identify different particles. Electrons are identified mainly using the information of the electromagnetic calorimeters and the specific energy loss by ionization in the Time Projection Chamber (TPC). Photons are identified mainly using the information from the electromagnetic calorimeters. In the case of photon conversion before the electromagnetic calorimeters the resulting e^+e^- pair can be detected by the tracking system. Penetrating muons can be identified by specialized muon detectors far from the interaction point. The reconstruction of secondary vertexes allows one to identify displaced vertexes from the decay of long-lived particles. The lifetime tag, based on the determination of secondary vertexes with a microvertex detector, is a fundamental tool for the beauty and charm identification. Anyway it has a limited power in the separation of charm from beauty events and hadron identification can help. Hadron identification is necessary to tag primary strange quark production. The identification of long-lived neutral particles is more challenging as they are seen in the calorimeters, having a worse resolution than tracking detectors. Neutral hadrons can be detected by the calorimeters, π^0 by the electromagnetic calorimeters and K^0_L and neutrons by the hadronic calorimeters.

Finally the RICH technique can provide charged particle identification over a large momentum range. A charged particle crossing a dielectric medium with a velocity larger than the speed of light in the medium emits photons at an angle θ_c (the Cherenkov angle) given by the relations

$$\cos\theta_c = \frac{1}{n\beta} \qquad \Longrightarrow \qquad m^2 = p^2\left[n^2\cos^2\theta - 1\right] \tag{1}$$

where $\beta = v/c$ and $n = n(E)$ is the refractive index of the medium,[3] in general dependent on the energy E of the emitted photon. The measurement of the speed of the particle, provided by the observation of the Cherenkov radiation, together with the measurement of the momentum of the particle by means of the tracking system, allows to estimate the particle mass, that is to identify the particle.

Among charged particles only electrons, muons, pions, kaons and protons have, in the conditions of the LEP collider, a decay length of the order or larger than the dimensions of the detectors. The particle identification of the DELPHI RICH is mainly a hadron identification, allowing to separate protons, kaons and pions. Pions can hardly be separated from muons and electrons by the RICH detector only, and the use of electron and muon identification is therefore required. A very useful information is provided by the cross-check between the RICH and the TPC identification.[4]

3 The Ring Imaging Cherenkov detector of DELPHI

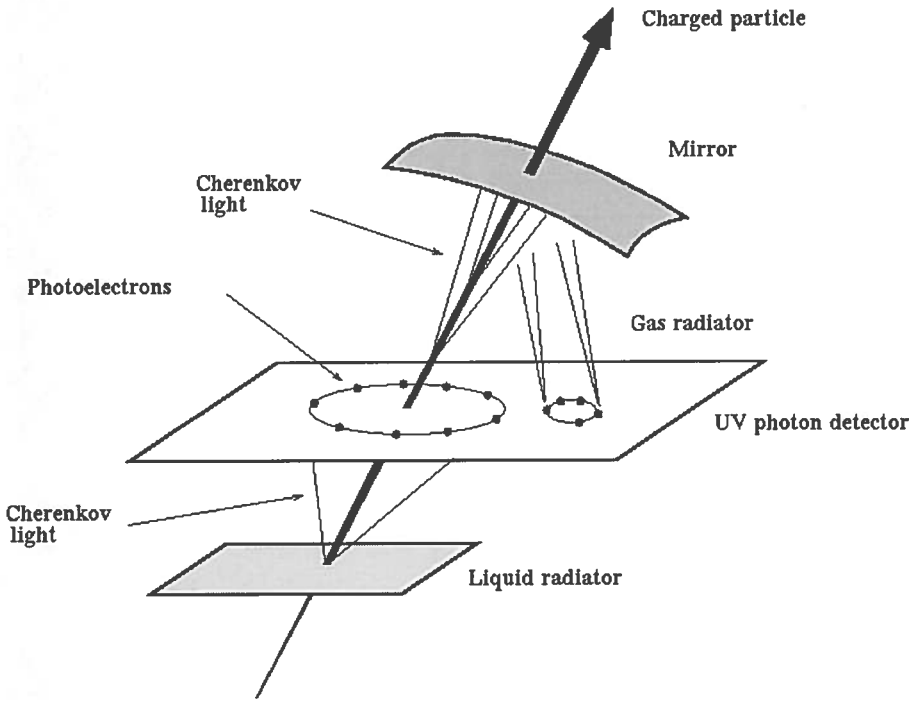

Figure 1: The DELPHI RICH operating principle.

The DELPHI RICH system is designed to provide charged particle identification, with an almost full coverage of the solid angle, for momenta above 0.7 GeV and up to the highest kinematically allowed momenta. The RICH detector is made of two parts. The cylindrical barrel part of the detector, the Barrel RICH, covers the polar angles $43° \leq \theta \leq 137°$ while the end-cap regions are covered by the Forward RICH in the polar angle regions $15° \leq \theta \leq 35°$ and $145° \leq \theta \leq 165°$.

RICHes are not standalone detectors but use the tracking information provided by the tracking detectors. In DELPHI tracking detectors are located just in front and behind the RICH, to provide precise tracking information at the entrance and exit of the RICH detectors. These detectors are the Time Projection Chamber (TPC) and Outer Detector (OD), in the barrel region, and the Forward Chamber A (FCA) and Forward Chamber B (FCB), in the end-cap regions. The DELPHI tracking system is completed by the tracking detectors closest to the interaction point: the Micro-Vertex detector (VD), the Inner Detector (ID) and the Very Forward Tracker (VFT).

The operating principle of the DELPHI RICH detector is shown in figure 1. Charged particle identification with the DELPHI RICH detector is obtained by using two different radiators, a liquid and a gas radiator, with different refractive index to cover a larger momentum range. Perfluorocarbons are used as radiators thanks to their ultraviolet transparency, low chromatic dispersion, non flammability, non toxicity and low chemical reactivity. The liquid radiator is C_6F_{14}. As a gas radiator C_4F_{10} has been chosen in the forward part while C_5F_{12} is used in the barrel part. The latter requires heating of the barrel detector to 40 °C because its boiling temperature is 28 °C. A charged particle crossing the detector first meets the liquid radiator and the emitted Cherenkov photons are directly detected by the photon detector. The Cherenkov photons produced by the particle going through the gas radiator are reflected and focused back onto the photon detector by a set of mirrors.

Cherenkov photons from the two radiators reach the photon detector on the two opposite sides, allowing to discriminate between the Cherenkov photons from the gas and from the liquid radiator. The photon detector is a photo-sensitive Time Projection Chamber providing a tri-dimensional reconstruction of the photon conversion point. Photons ionize the TMAE by photoelectric effect and the photoelectrons drift under the effect of the electric drift field onto a set of Multi-Wire Proportional Chambers used for the readout. The photosensitive agent is TMAE,[5] which is chosen for its low ionization energy and high quantum efficiency. The use of TMAE as a photosensitive agent allows to use cheap quartz windows. The ionization signal produced by the charged particle while it crosses the photon detector is also detected and used to provide one more track element to the DELPHI tracking system. Single photoelectron sensitivity is required and a very low contamination from electronegative elements (like water and oxygen) is therefore required. Feedback photons produced in the avalanche multiplication process might ionize the TMAE. They are suppressed by a set of suitable screens located on the Multi-Wire Proportional Chambers. The Cherenkov radiators transparency is well matched to the TMAE sensitive interval and quartz wavelength cut-off.

Particle identification with a RICH detector exploits both the threshold characteristics and the dependence of the Cherenkov angle and number of emitted photons on the particle velocity. The analysis is done for both radiators by looking for Cherenkov photons detected at a given angle from a charged track of known momentum. Depending on the particle momentum and mass a well defined Cherenkov angle is expected for the photons from all the particles above the Cherenkov threshold and no photons in case the particle momentum is below the threshold. In the first case (ring identification) the measured Cherenkov angle is compared with the expected angle for all particle hypothesis. In the second case (veto identification) the particle identification with a given radiator may be ambiguous because it cannot discriminate among all the particles giving no Cherenkov light.

In the high momentum region the gas radiator information is mainly used while in the low momentum region the liquid radiator information is more useful. The information from the two radiators is combined, to help the identification especially in the intermediate momentum region.

The DELPHI RICH system can provide pion-kaon separation up to about 25 GeV momentum and kaon-proton separation up to about 35 GeV momentum, the exact limits depending on the specific analysis.

4 Particle identification in physics analysis

Many topics can benefit from a reliable charged particle identification capability, both at LEP I and at the high energy LEP200 phase of the LEP collider. The most important topics which have benefited by the charged particle identification capability provided by the RICH detector are summarized below.

- Physics at LEP I
  - Tau physics: τ-lepton decays into strange mesons.
  - Beauty physics.
  - Bose-Einstein correlations of charged kaons.
  - Electroweak physics: strange quark forward-backward asymmetry (and cross section).
  - QCD: charged particle production in hadronic events.
- Physics at LEP 200

- Cross section and asymmetry for identified fermions.
- Search for long-lived heavy charged particles.
- Determination of $\left|V_{cs}^{CKM}\right|$.
- QCD: evolution of the physical quantities as a function of the energy.
- Beauty tagging at LEP200 (important in Higgs boson searches).

Very good, although old, summaries of the RICH technique, including reports on physics results, can be found in the Proceedings of the first two International Workshops on Ring Imaging Cherenkov Detectors held during 1992 in Bari and during 1995 in Uppsala.[6,7]

5 Particle identification at LEP I

5.1 Tau lepton physics

One important item in τ-lepton physics is the measurement of the τ-lepton branching ratios into final states containing strange mesons. These measurements, requiring a very good kaon-pion separation, can check the Standard Model predictions and may provide potential information on new physics.

DELPHI has measured the $\tau \to \mathrm{K}\nu_\tau$ and $\tau \to \mathrm{K}^*(892)\nu_\tau$ branching ratios, by exploiting the particle identification capability provided by its RICH detector, to extract the signal from the much larger background due to the $\tau \to \pi\nu_\tau$ events.[8,9] A very good rejection factor is required due to the much higher yield of pions compared to (Cabibbo suppressed) kaons in the τ decay. Results from the 1993-1994 data are the following

$$\tau \to \mathrm{K}\nu_\tau = 0.76 \pm 0.08\ (\mathrm{stat.}) \pm 0.02\ (\mathrm{syst.})\% \quad (2)$$

$$\tau \to \pi\nu_\tau = 10.5 \pm 0.1\ (\mathrm{stat.}) \pm 0.2\ (\mathrm{syst.})\% \quad (3)$$

The precision is comparable with the best published results and the understanding of systematics errors is good. The measurements are limited by statistics and compatible with the Standard Model theoretical predictions.

The measurement of the branching ratios of the three-prongs $\tau \to \mathrm{KK}\pi\nu_\tau$ and $\tau \to \mathrm{K}\pi\pi\nu_\tau$ decays is more challenging. In fact the high momentum of the τ from the Z^0 decay produces three highly collimated and high momentum particles. The ring reconstruction is therefore particularly difficult because the rings overlap. The branching ratios were nevertheless measured for the channels $\tau \to \pi\pi\pi(\geq 0\pi^0)\,\nu_\tau$, $\tau \to \mathrm{K}\pi\pi(\geq 0\pi^0)\,\nu_\tau$ and $\tau \to \mathrm{KK}\pi(\geq 0\pi^0)\,\nu_\tau$. Preliminary results for the data collected by the DELPHI experiment in 1993-1995 are shown in table 5.1.[10] The results are compatible with already published data but their precision is superior. The measurements are in good agreement with the theoretical predictions for the Cabibbo allowed modes while a significant discrepancy appears in the channel $\mathrm{K}\pi\pi(\geq 0\pi^0)\,\nu_\tau$ possibly due to uncertainty on the width of the $\mathrm{K}_1(1270)$ and $\mathrm{K}_1(1400)$ resonances used in the theoretical calculations.

Channel	Branching ratio %
$\pi\pi\pi(\geq 0\pi^0)\,\nu_\tau$	$13.77 \pm 0.04 \pm 0.13$
$\mathrm{K}\pi\pi(\geq 0\pi^0)\,\nu_\tau$	$0.33 \pm 0.04 \pm 0.02$
$\mathrm{KK}\pi(\geq 0\pi^0)\,\nu_\tau$	$0.24 \pm 0.04 \pm 0.03$

The $\tau \to \mathrm{KK}\pi\nu_\tau$ channel is particularly interesting because it is well suited to set a limit on the ν_τ mass, due to the high total mass of the final hadronic state. In figure 2 a reconstructed $\tau \to \mathrm{KK}\pi\nu_\tau$ event is shown with the pion and kaons identified by the RICH.

The absence of protons among the τ decay products is an interesting feature which can be exploited in $e^+e^- \to \tau^+\tau^-$ events. This characteristic can in fact be used to study and tune the particle identification methods, by studying the probability to misidentify pions and kaons as protons.

5.2 Beauty physics

The RICH is extensively used in beauty physics (see[11] and references therein). The analysis in the field of beauty physics are particularly interesting because they test the potential of a RICH detector, for a possible use at the future beauty factories, designed to study CP violation and rare decays in the beauty system.

Kaon identification in fully reconstructed events allowed a precise determination of the B_s^0 mass. The lifetime of the Λ_b^0 was measured using proton or kaon identification information from the RICH. Rare B decays were reconstructed by using the precise information from the tracking system and the particle identification capabilities provided by the RICH. Evidence for charmless B decays has been obtained. Also evidence for new B particles has been obtained using the RICH, like the B^{**} and B_s^{**}. An example of a beauty event reconstructed by using the hadron identification capabilities is shown in figure 3.

At LEP200 the beauty tagging is particularly important due to its usefulness in the Higgs boson searches, as in the LEP200 energy region the Higgs mainly decays into a $b\bar{b}$ pair.

5.3 Charged kaon interference in hadronic Z^0 decays

Correlations between identical pions have been studied extensively in different types of reactions. An enhancement at small relative momenta is attributed to the Bose-Einstein effect. The interference between neutral kaons has also revealed the influence of the Bose-Einstein statistics.

The first measurement of like-sign charged kaon correlations in hadronic e^+e^- annihilation at the Z^0 mass was presented in.[12] The charged kaons are identified by means of the RICH detector with a purity of about 70%, as estimated from the simulation. A sample of about $1 \cdot 10^6$ events was selected in 1994 DELPHI data with the RICH detector fully operational. About $1.1 \cdot 10^5$ events have at least two charged kaons. A significant enhancement at small values of the four-momentum difference is observed in the ratio of like-sign to unlike-sign KK pairs and in the ratio of like-sign pairs to a simulated reference sample. This is attributed to the Bose-Einstein interference effect between identical bosons. The measured Bose-Einstein correlation parameters λ and r are similar for charged and neutral kaon pairs. and the value of the Bose-Einstein correlation strength λ is consistent with unity.

5.4 Stange particles tagging ($s\bar{s}$ asymmetry and cross section)

The main process studied at LEP is the e^+e^- annihilation process $e^+e^- \to f\bar{f}$. The final state fermion is a quark in about 70% of the cases and many physical measurements rely on the identification of the flavour of the primary quark. The tagging of a primary strange quark allows the measurement of the Z^0 decay width into strange quarks pairs, $\Gamma_{s\bar{s}}$, and the strange quark forward backward asymmetry, A_{FB}^s. Comparing the measurements for the different quark flavors allows one to test the universality of the electroweak couplings and provide additional data as input to the fit to theoretical models.

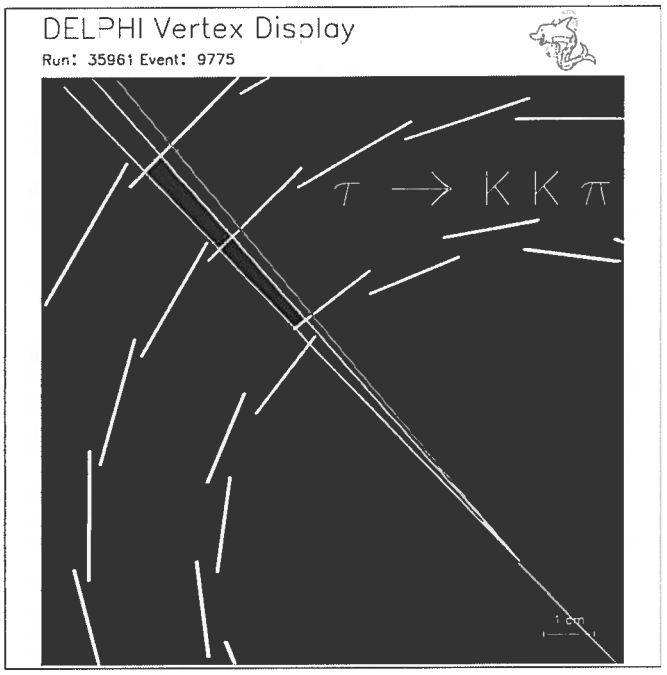

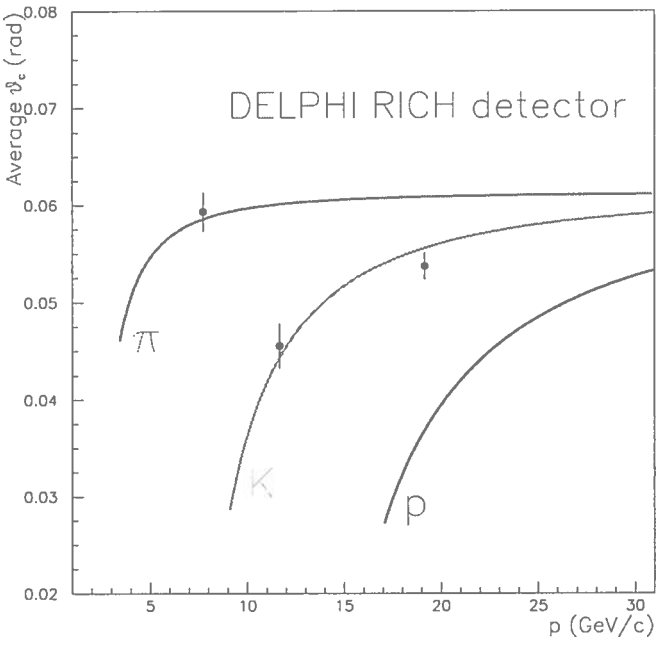

Figure 2: A $\tau \to \mathrm{KK}\pi\nu_\tau$ event. The pion and the kaons are identified by the RICH.

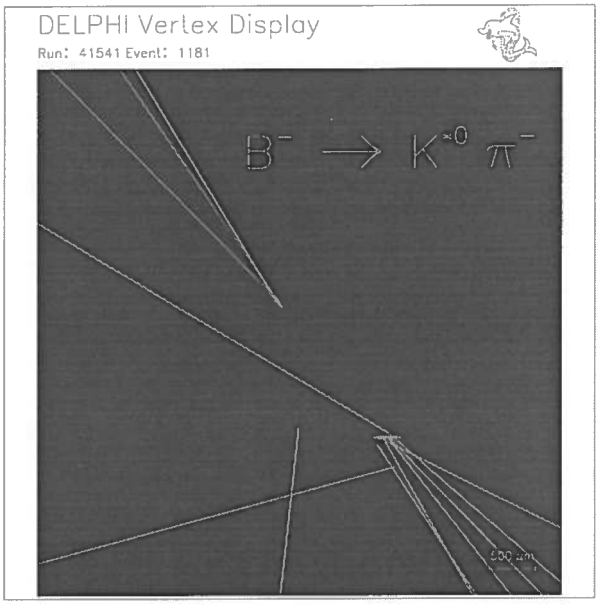

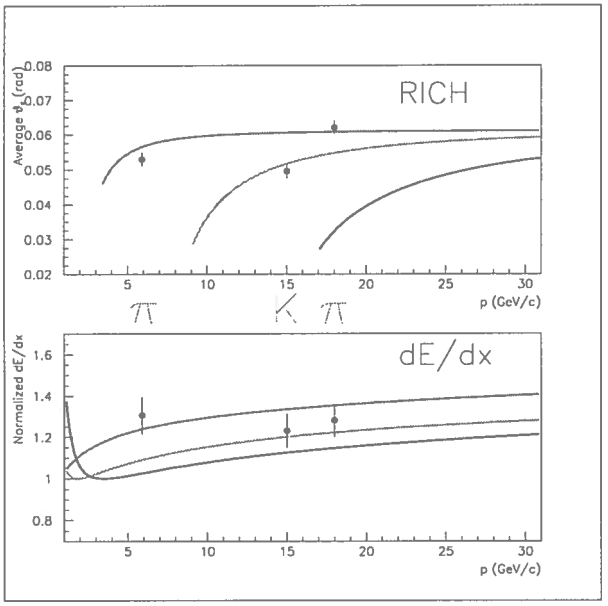

Figure 3: The use of the RICH and $\mathrm{d}E/\mathrm{d}x$ particle identification in beauty physics.

The primary strange quark can be tagged by looking for high momentum final state strange mesons and baryons. The main background to this process comes from strange hadrons produced in the fragmentation and from decays of heavy flavors. Strange final state particles are therefore not a unique signature of a strange primary quark. The requirement of high momentum allows to increase the purity of the tagging because the primary quarks tend to keep a larger fraction of the initial momentum. In principle any strange hadron is suitable to tag primary strange quarks but in practice kaons are favoured by the higher statistics and, the charged ones, by the possibility to identify them with high efficiency. The meson electric charge or the baryonic number of the baryon allow to separate the s quark from the $\bar{s}$ anti-quark. The RICH can be used to tag the high momentum kaons by means of the gas radiator information only as the emphasis is in the tagging of high momentum particles.

5.4.1 Measurement of the $s\bar{s}$ asymmetry

The angular dependence of the differential cross section for the $e^+e^- \to f\bar{f}$ process, for unpolarized e^+e^- beams at the Z^0 peak and at the lowest perturbative level, is given by

$$\frac{d\sigma^f}{d\cos\theta}(s) = \sigma^f(s)\left[\frac{3}{8}\left(1+\cos^2\theta\right) + A^f_{FB}(s)\cos\theta\right] \tag{4}$$

where θ is the polar angle between the incoming electron and the outgoing fermion, s is the squared center of mass energy and the term $A^f_{FB}(s)$ corresponds to the forward-backward fermion asymmetry,

$$A^f_{FB}(s) = \frac{\sigma_F - \sigma_B}{\sigma_F + \sigma_B} \tag{5}$$

which is energy dependent. In the formula above the fermion f can be any fermion but the electron because in the case of the electron the t-channel exchange must be included. Radiative corrections, which modify the lowest order predictions, must be taken into account when comparing the theoretical predictions with data in precision measurements.

High energy charged kaons with momentum in the range of $10\ \text{GeV} \lesssim p \lesssim 24\ \text{GeV}$, can be identified by means of the RICH detector and used to measure the strange quark forward backward asymmetry.[13] The forward region is especially important in the $s\bar{s}$ asymmetry measurement because the polar angle distribution of the differential cross section gives a maximum asymmetry in the forward regions.

The main difficulty to the determination of the strange quark asymmetry is to have a reliable identification of the jet flavour and jet charge, as in all others quark asymmetry measurements. An additional complication in strange quark tagging, as compared to the beauty quark one, is the contamination from strange particles coming from the parton shower and from heavy flavour decays.

One important item to take into account in the asymmetry measurement is the fact that the detector is not perfectly symmetrical mainly because of slightly different operating conditions, like for instance tripping chambers, slightly different efficiencies, etc. To avoid this problem the asymmetry between the number of events with negative and positive kaons in the same angular region is computed, instead of the asymmetry between kaons of the same charge in opposite angular regions. This allows to avoid the estimation of the relative detection efficiency of the kaons tagging strange quarks and anti-quarks which is due to detector material inhomogeneity and to different detector operation in opposite hemispheres. The calculation of the selection efficiency is not necessary because any efficiency factor cancel in the ratio.

After defining the criteria to select a good track, hadronic events are selected according to the usual selection rules: a large enough number of charged particles, a large enough energy associated with charged tracks, both in the whole event and in each of the two hemispheres, defined according to the thrust axis with all particles considered as pions. The residual contamination from $Z^0 \to \tau^+\tau^-$ and $Z^0 \to \gamma\gamma$ is estimated to be less than 0.3% and the contamination coming from beam gas interaction to be less than 0.1%.

The particles identified as kaons have to be inside the RICH geometrical acceptance, have a momentum $10 \text{ GeV} \lesssim p \lesssim 24 \text{ GeV}$ and at least two detected photoelectrons are required in order to reconstruct the Cherenkov angle. The lower momentum limit is imposed by the Cherenkov emission threshold in the gas radiator while the upper momentum limit is imposed by the requirement to have a one standard deviation separation between pions and kaons. In case more than one kaon with this characteristics are found in the event the most energetic one is selected. The direction of the primary quark can be estimated by the thrust axis of the event.

Analysis method. Two methods are available for the measurement: a track by track identification and a statistical separation method where single tracks are not identified but the overall squared mass distribution is analyzed and fitted to the kaon and pion contribution to provide the sample composition.

In the statistical method the m^2 distribution is fitted by the sum of two Breit-Wigner distributions representing the kaon contribution and the pion (plus electron and muon) contribution, as shown in figure 4. The fit provides the total number of kaons in the sample and has the advantage that no estimate of the kaon selection efficiency and purity is required.

The track by track identification method is based on the individual track identification. A kaon selection based on the measured mean Cherenkov angle provides and average selection efficiency of about 53% in the barrel region and about 42% in the forward region, according to simulation. The selection of events with high momentum kaons gives a selected sample consisting of about 43% events originating from a primary strange quark. The purity of the kaon sample can be further increased using a beauty quark tagging to remove beauty events. In this way the strange quark events fraction can be increased from about 43% to about 55%. The beauty events rejection cannot be applied in the forward region of the detector because this is outside the acceptance of the microvertex detector used in the beauty quark tagging.

The measurement of the kaon asymmetry is done assuming the theoretical behavior of the asymmetry as a function of the quark polar angle and fitting the measured distribution to the theoretical one.

The asymmetry has to be corrected for the purity of the kaon sample (pions misidentified as kaons) and the asymmetry due to different interaction cross section of positive and negative kaons. Both corrections depend of the polar angle. The material asymmetry is to a first approximation proportional to the material length crossed and was computed to correct for the different interaction cross sections of positive and negative charged kaons. It was estimated using a full Monte Carlo simulation and was found to be less than 2% at any polar angle. The kaon purity was obtained from the full simulation and has the average value of about 84% in the barrel and 74% in the forward region.

Results. Corrections have to be applied to take into account the contamination of the sample from other flavors, the possible wrong definition of the primary quark charge and the uncertainty in the estimation of the quark direction by the thrust axis.

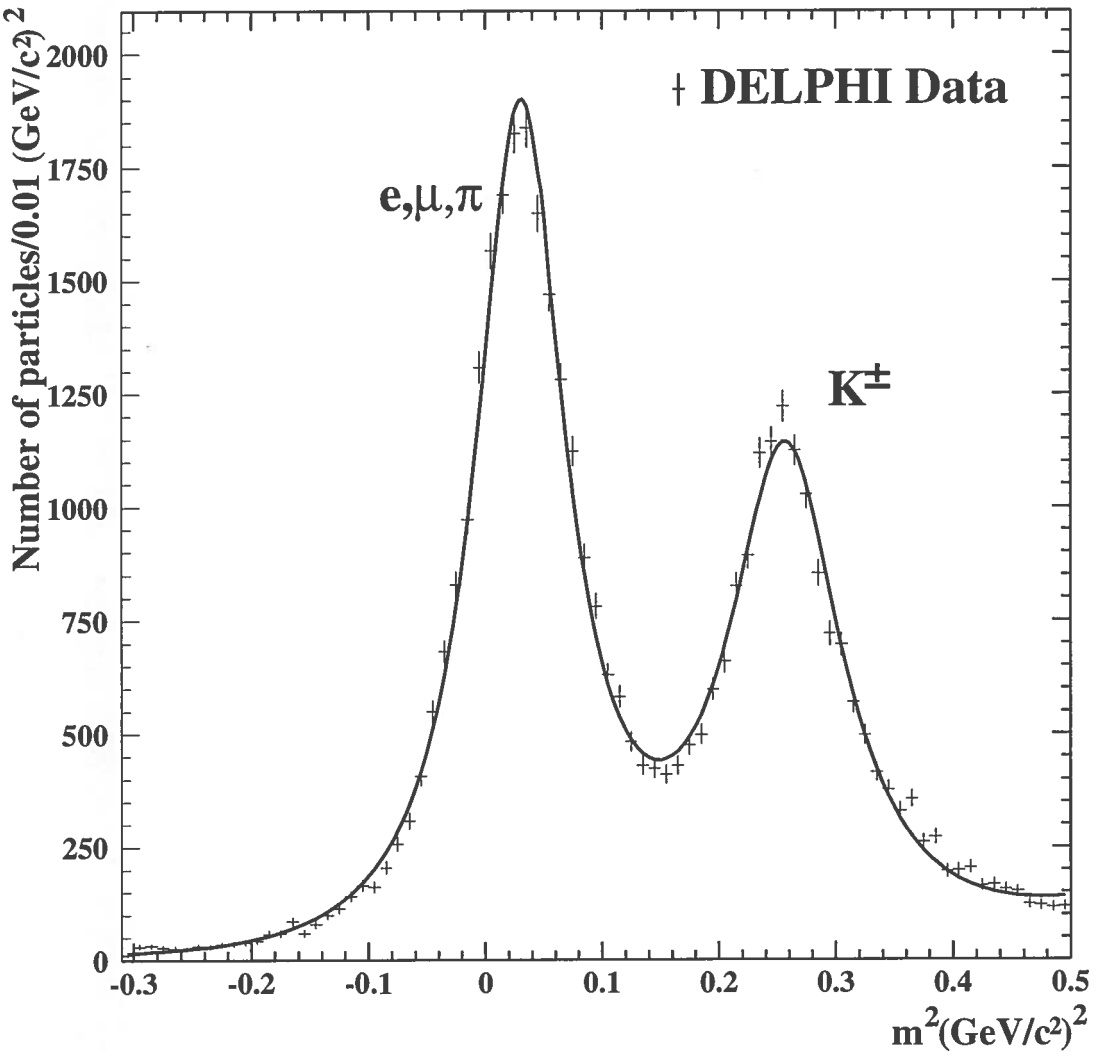

Figure 4: Charged particles with 10 GeV $< p <$ 18 GeV.

From the kaon asymmetry, depending on all the kaons in the sample, not only those originating from a primary strange quark, it is possible to extract the strange quark asymmetry as the measured kaon asymmetry is a linear combination of the asymmetry of the primary quark flavors.

The pole asymmetry A^s_{FB}, measured using $1.4 \cdot 10^6$ hadronic Z^0 events collected in 1994, was found to be

$$A^s_{FB} = 0.114 \pm 0.019 \text{ (stat.)} \pm 0.005 \text{ (syst.)} \quad (6)$$

The measurements is consistent with universality of the strange and bottom quarks couplings. A similar measurement has been recently done also by the OPAL and SLC collaborations[14,15] providing compatible results.

5.5 QCD

The understanding of the process of the fragmentation of coloured partons into colorless hadrons is one of the most important issues of QCD. The measurement of the identity of hadronic final state particles in e^+e^- annihilation is fundamental to the understanding of the fragmentation of quarks and gluons into hadrons.

The process of hadron production in e^+e^- annihilation can be split into four phases. The first phase is the electroweak e^+e^- annihilation into a Z^0 or γ, with initial state radiation emission, and production of the primary quark-antiquark pair. In the second phase gluon radiation and gluon splitting are modeled. The third phase is the hadronization of the partons into final state hadrons. In the fourth phase the final state hadrons are allowed to decay. The second phase, the hard QCD process, that is the formation of quarks and gluons, is properly described by perturbative QCD. On the other hand the hadronization phase, during which the transition between partons and hadrons occurs, cannot be described by perturbative methods because the small momentum transfers implies a large strong coupling constant. One has then to rely on phenomenological models to describe the transition from partons to hadrons.[16,17] It is therefore important to compare with the data the predictions of the models to tune the phenomenological models.

The measurement of identified particle spectra can be used to improve, test, differentiate and tune the models used to describe the parton cascade and the transition from partons to final state hadrons. Two models are commonly used to describe the fragmentation, the string and the cluster models. The string model usually fits the data better the the cluster model but the latter has a lower number of free parameters.

Multihadronic events originate from the production of a quark-antiquark pair, possibly with subsequent gluon and additional quarks radiation. The observation that hadrons are collimated in jets indicates a duality between partons and final state hadrons. It can be further postulated that this duality is local, that is the hadron cross sections are proportional to those at the parton level (LPHD). Together with the Modified Leading Logarithm Approximation (MLLA) this allows a prediction of the hadronic cross section.[18]

5.5.1 Production of $\pi^\pm$, $K^\pm$ and $p\bar{p}$ at LEP I

DELPHI has measured the pion, kaon and proton production rates, differential cross-sections and multiplicities in $1.4 \cdot 10^6$ hadronic Z^0 events collected in 1994. The measurements were carried on three different samples: $Z^0 \to q\bar{q}$, $Z^0 \to b\bar{b}$ and a light quark enriched sample, $Z^0 \to \left[u\bar{u} \oplus d\bar{d} \oplus s\bar{s}\right]$. The results can be compared with the predictions of the JETSET[16]

string fragmentation model and the HERWIG[17] cluster fragmentation model, both of them tuned by the DELPHI experiment.

The particle identification capability provided by the RICH detector are an essential tool in the study of identified particles in hadronic events. Some of the results show a substantial improvement in accuracy compared to previous measurements and some results are presented for the first time.[19]

Tagging $Z^0 \to q\bar{q}$, $Z^0 \to b\bar{b}$ and $Z^0 \to \left[u\bar{u} \oplus d\bar{d} \oplus s\bar{s}\right]$ events. To select b-flavored and uds-flavored enriched samples a topological lifetime b-tagging was applied. The method defines an event probability based on the positive lifetime-signed impact parameter significance of all the tracks of the event consistent with the primary vertex. The probability can be used to select or suppress beauty events. The impact parameter is defined as the minimum distance between the reconstructed track trajectory and the reconstructed primary vertex. The sign is defined with respect to the jet direction which implies the sign to be positive if the vector joining the primary vertex and the point of closest approach of the track to the primary vertex has a positive projection on the jet axis to which it belongs. The significance of the track is defined as the ratio between the impact parameter and its error, the latter depending on the accuracy of the tracking system. The negative part of the significance distribution is only sensitive to detector resolution effects and it is therefore used to compute, from the data themselves, a significance probability density for tracks coming from the primary vertex. The method is based on the fact that beauty hadrons usually have long lifetime and large mass and energy. The average decay length, of the order of a few millimeters, and the large rest mass of the hadron produce decay products with large impact parameter.

Method. The real particle content of a sample is obtained from the measured number of particles through the tagging efficiency matrix

$$\begin{pmatrix} N_\pi \\ N_\mathrm{K} \\ N_\mathrm{p} \end{pmatrix}^{\mathrm{Meas}}(x) = \begin{pmatrix} \mathcal{E}_\pi^\pi & \mathcal{E}_\mathrm{K}^\pi & \mathcal{E}_\mathrm{p}^\pi \\ \mathcal{E}_\pi^\mathrm{K} & \mathcal{E}_\mathrm{K}^\mathrm{K} & \mathcal{E}_\mathrm{p}^\mathrm{K} \\ \mathcal{E}_\pi^\mathrm{p} & \mathcal{E}_\mathrm{K}^\mathrm{p} & \mathcal{E}_\mathrm{p}^\mathrm{p} \end{pmatrix} \cdot \begin{pmatrix} N_\pi \\ N_\mathrm{K} \\ N_\mathrm{p} \end{pmatrix}^{\mathrm{Real}}(x) \tag{7}$$

where, for $i, j = \pi$, K, p, the vector element N_i stands for the normalized number of particles of type i and the matrix element $\mathcal{E}_i^j$ represents the efficiency of tagging a particle of true identity i as a particle of type j. The tagging efficiency matrix is derived from the simulation. In principle, any observable can be taken for x like the momentum p, $X_p = p/p_{\mathrm{beam}}$, $\xi_p = -\ln X_p$ or the rapidity y. The method implicitly accounts for particle misidentification, provided the full detector simulation describes the data well. The real data content may be obtained either by matrix inversion or by using a more robust estimation method, especially in cases when statistics is low. Figure 5 illustrates the tagging efficiency matrix for a standard hadron tag and a very loose track selection as a function of momentum in equation 7.

In the momentum window between 2.7 and 8.5 GeV/c two options are available for tagging kaons and protons.[20] Either one can choose positive identification for both $\mathrm{K}^\pm$ and $\mathrm{p\bar{p}}$ through the combined use of liquid and gas radiator information, or one can choose not to distinguish $\mathrm{K}^\pm$ from $\mathrm{p\bar{p}}$ by using only the gas radiator veto-information, the so called heavy particle tag. Heavy particles $\mathrm{Hv}^\pm$ are defined as particles which are heavier than pions.

The efficiency matrix is estimated using Monte Carlo but can be, at least in part, tested on real data, provided one has a sample of particles tagged by an independent method.

At low momenta ($p < 1.3$ GeV/c), the proton tag is based on the RICH liquid veto-information which has a low efficiency, due to the large number of photons in the liquid. The efficiency can

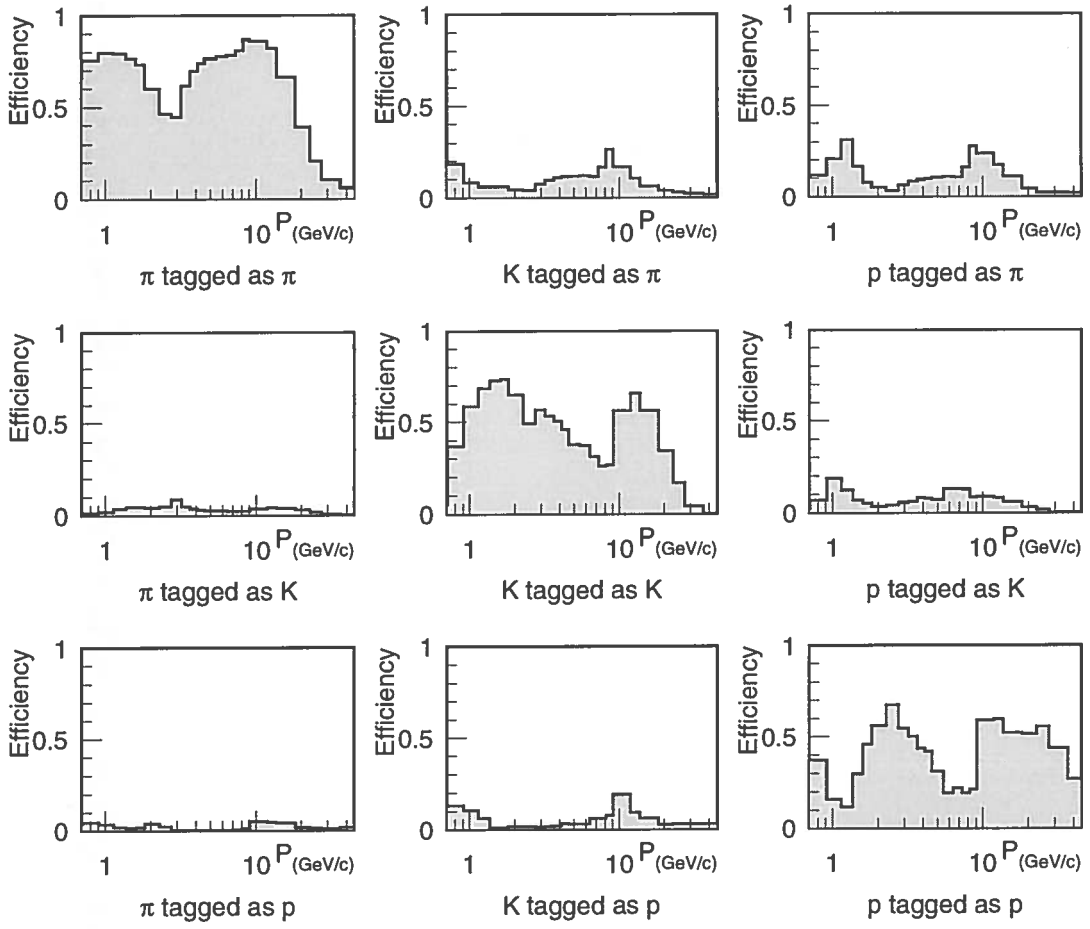

Figure 5: The tagging efficiency matrix for standard output and very loose selected tracks versus momentum (for tracks with Outer Detector information).

be increased by using also the $\mathrm{d}E/\mathrm{d}x$ measurement in the TPC, defining similar tagging and track quality levels.

The agreement between data and Monte Carlo was checked using pions from $\mathrm{K}^0_\mathrm{S} \to \pi^+\pi^-$ and protons from $\Lambda^0 \to \mathrm{p}\pi^-$ decays, as shown in figure 6. The pion purity was estimated from the K^0_S sample to be $\sim 94\%$ and the proton purity from the Λ^0 sample to be $\sim 75\%$. The right-hand side of the figure appears to show that a proton is more likely to be misidentified as a pion than as a kaon. This can be understood from the low purity of the proton sample. The dashed lines in the right-hand side column represent the correctly tagged part of the Monte Carlo, e.g. the dashed line in the top right plot (proton tagged as pion) represents real pions which the Λ^0 reconstruction indicated were protons. The detector simulation describes the data well.

Results on the normalized production rates. Due to the high statistics, the systematic uncertainties usually dominate. Preliminary results on the normalized $\pi^\pm$, $\mathrm{K}^\pm$ and $\mathrm{p\bar{p}}$ production rates, derived from the matrix method for the $\mathrm{Z}^0 \to \mathrm{q\bar{q}}$, $\mathrm{Z}^0 \to \mathrm{b\bar{b}}$ and $\mathrm{Z}^0 \to \left[\mathrm{u\bar{u}} \oplus \mathrm{d\bar{d}} \oplus \mathrm{s\bar{s}}\right]$ samples, are shown in figure 7. For all three event samples, JETSET turns out to give a good description of the data. For $\pi^\pm$ and $\mathrm{K}^\pm$ in $\mathrm{Z}^0 \to \mathrm{q\bar{q}}$ and for $\mathrm{K}^\pm$ in $\mathrm{Z}^0 \to \left[\mathrm{u\bar{u}} \oplus \mathrm{d\bar{d}} \oplus \mathrm{s\bar{s}}\right]$ events, the HERWIG prediction is also good. However in all other cases HERWIG seems to fail, especially for protons. The production rates from this analysis compared to published results from other sources are shown in

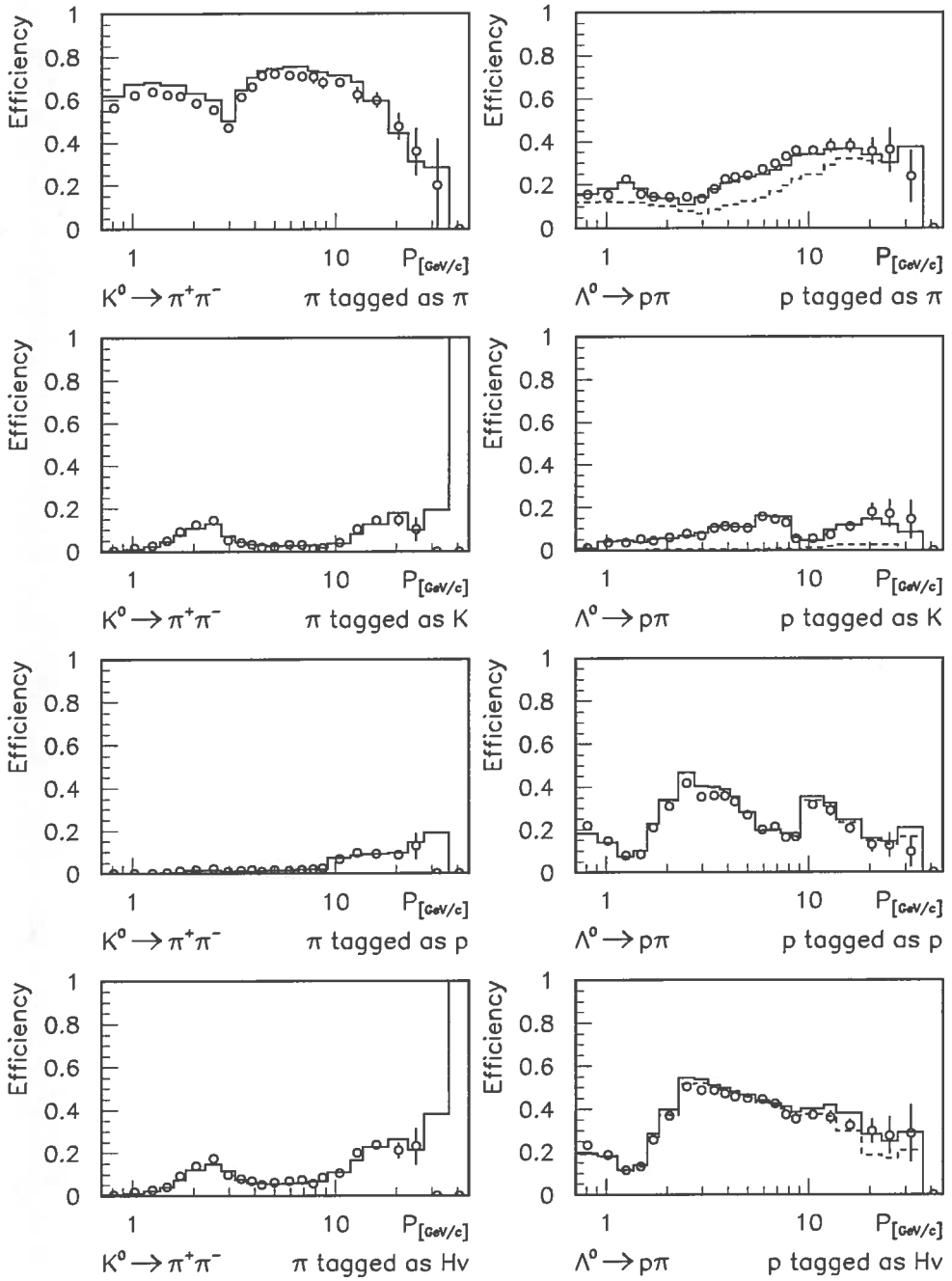

Figure 6: Agreement between data and Monte Carlo using pions from $K^0_S \to \pi^+\pi^-$ and protons from $\Lambda^0 \to p\pi^-$ decays.

table 1.

$Z^0 \to q\bar{q}$	DELPHI	ϵ_{tot}	OTHERS	ϵ_{tot}		$\triangle\epsilon$
$< n_q >$	20.81	± 0.44	20.92	± 0.24	LEP Av.[21]	0.22
$< \pi^{\pm} >$	17.26	± 1.17	17.1	± 0.4	PDG'96[22]	0.13
			17.052	± 0.429	OPAL[23]	0.17
$< K^{\pm} >$	2.21	± 0.08	2.39	± 0.12	PDG'96[22]	1.25
			2.421	± 0.133	OPAL[23]	1.36
			2.26	± 0.18	DELPHI[24]	0.25
$< p\bar{p} >$	1.08	± 0.05	0.964	± 0.102	PDG'96[22]	1.02
			0.916	± 0.111	OPAL[23]	1.35
			1.07	± 0.14	DELPHI[24]	0.07
$Z^0 \to b\bar{b}$	DELPHI	ϵ_{tot}	OTHERS	ϵ_{tot}		$\triangle\epsilon$
$< n_b >$	23.17	± 0.46	23.47	± 0.37	DELPHI[26]	0.51
			23.62	± 0.48	OPAL[27]	0.68
			23.14	± 0.39	SLD[28]	0.05
$< K^{\pm} >$	2.59	± 0.10	2.74	± 0.50	DELPHI[25]	0.29
$< p\bar{p} >$	1.07	± 0.07	1.13	± 0.26	DELPHI[25]	0.22
$Z^0 \to \boxed{u\bar{u} \oplus d\bar{d} \oplus s\bar{s}}$	DELPHI	ϵ_{tot}	OTHERS	ϵ_{tot}		$\triangle\epsilon$
$< n_{uds} >$	19.94	± 0.42	20.35	± 0.19	DELPHI[26]	0.89
			20.21	± 0.24	SLD[28]	0.56

Table 1: The production rates from this analysis compared to published results from other sources. The measurements of $\pi^{\pm}$, $K^{\pm}$ and $p\bar{p}$ multiplicities in $Z^0 \to b\bar{b}$ and $Z^0 \to \left[u\bar{u} \oplus d\bar{d} \oplus s\bar{s}\right]$ events at LEP have so far only been published by DELPHI. The column $\triangle\epsilon$ gives the difference in standard deviations between the measurements.

Results on the differential cross sections. Figure 8 shows preliminary results on the $\pi^{\pm}$, $K^{\pm}$ and $p\bar{p}$ differential cross-sections versus momentum (bottom, left hand axes) and versus scaled momentum X_p (top, right hand axes), for $Z^0 \to q\bar{q}$, $Z^0 \to b\bar{b}$ and $Z^0 \to \left[u\bar{u} \oplus d\bar{d} \oplus s\bar{s}\right]$ as obtained from the matrix method. For all three event samples, JETSET describes the measured spectra better than HERWIG, which fails to describe the proton spectra and generally over estimates the spectra for $Z^0 \to b\bar{b}$ and under estimates them for $Z^0 \to \left[u\bar{u} \oplus d\bar{d} \oplus s\bar{s}\right]$ events. The overall JETSET description is rather good.

Results on the particle multiplicity. The particle multiplicities, that id the total particle production rates, can be obtained by integrating the differential cross-section distribution of any observable e.g. p, X_p or ξ_p. The DELPHI particle multiplicities are determined through integration over the ξ_p range of the above presented distorted Gaussian fit-results. The JETSET prediction was used to extrapolate into the regions not covered by the data.

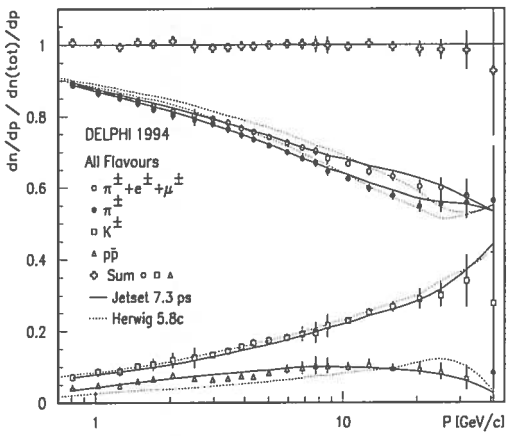

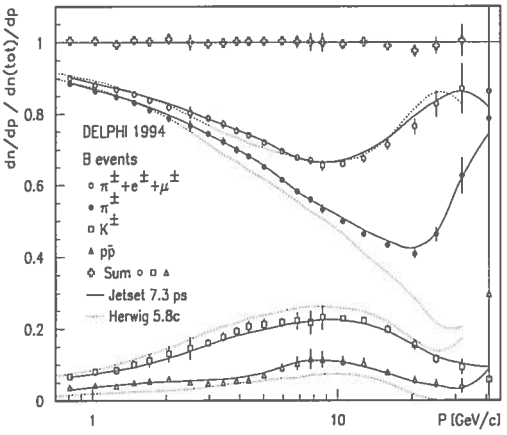

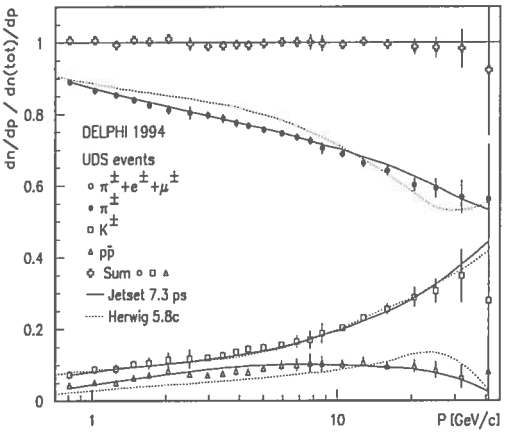

Figure 7: The normalized production rates of $\pi^{\pm}$, $K^{\pm}$ and $p\bar{p}$ in $Z^0 \to q\bar{q}$, $Z^0 \to b\bar{b}$ and $Z^0 \to [u\bar{u} \oplus d\bar{d} \oplus s\bar{s}]$. The open symbols are the measured distributions (acceptance corrected). The closed circles indicate $\pi^{\pm}$ after having accounted for $e^{\pm}$ and $\mu^{\pm}$. The distributions have been obtained without constraining the sum of the fractions to equal unity, allowing the consistency test indicated by the open crosses. Compared to $Z^0 \to [u\bar{u} \oplus d\bar{d} \oplus s\bar{s}]$, the production of high momentum $K^{\pm}$ ($p > 20$ GeV/c) is suppressed in b - events, whereas $K^{\pm}$ production for $3 < p < 20$ GeV/c is clearly higher in b - events.

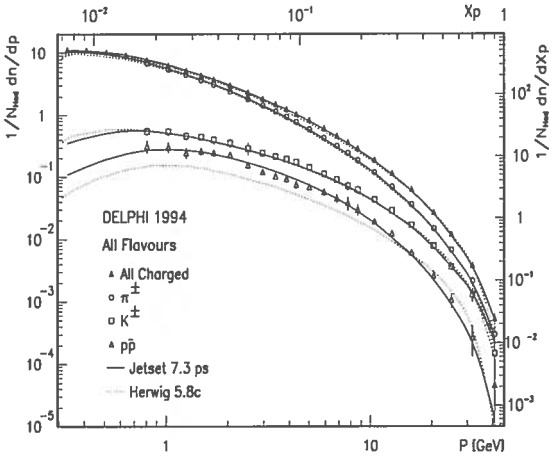

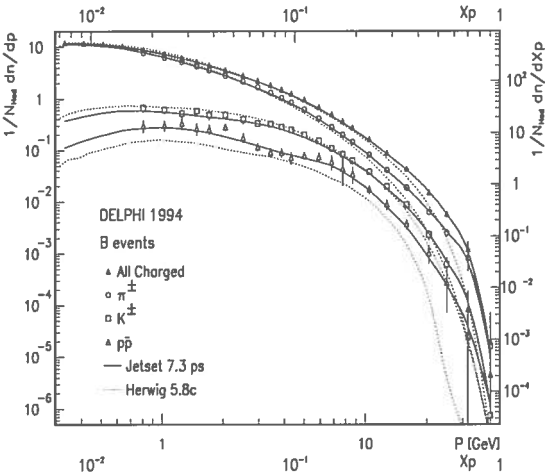

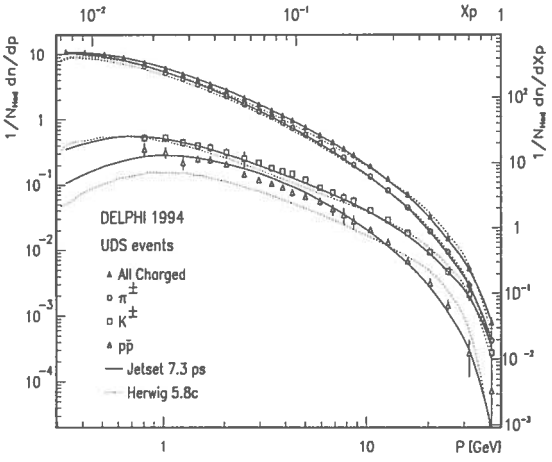

Figure 8: The differential cross-sections versus momentum (bottom and left hand axes) and versus the scaled momentum X_p (top and right hand axes), for $Z^0 \to q\bar{q}$, $Z^0 \to b\bar{b}$ and $Z^0 \to [u\bar{u} \oplus d\bar{d} \oplus s\bar{s}]$. The corresponding values and uncertainties are listed in.[19]

6 Particle identification at LEP 200

6.1 $\pi^{\pm}$, $K^{\pm}$, $p\bar{p}$ production at LEP200

The same analysis on charged particle multiplicity performed at LEP I is in progress with the LEP200 data even if the statistics is much lower than at LEP I. The analysis allows to test the running of physical quantities with the energy, which can be predicted in the framework of the MLLA plus LPHD.[18] The production of charged kaons and protons has been measured at energies above the Z^0 peak and the results on the average multiplicity of such identified particles and on the position of the ξ^* of the maximum of the ξ_p distribution have been compared with the predictions of JETSET and HERWIG Monte Carlo programs and with MLLA plus LPHD.[29] The Monte Carlo programs display in general a fair agreement with the data, in the limit of the little available statistics. Within the available statistics the shape of the ξ_p distribution is also well reproduced by the Monte Carlo programs as well as the evolution with the energy of the the position of the ξ^* of the maximum of the ξ_p distribution. More statistics is necessary to perform a stringent test.

6.2 Search for long-lived heavy charged particles.

A search for long-lived heavy charged particles in e^+e^- collision at a center of mass energy ranging from 130 GeV up to 172 GeV was performed by DELPHI. The search is based on particle identification provided by the specific ionization loss in the Time Projection Chamber and by the RICH. No candidate was observed and upper limits to the production cross sections for various kind of particles were set.[30]

6.3 Determination of $\left|V_{cs}^{CKM}\right|$

Measurement of $\left|V_{cs}^{CKM}\right|$ using W decays and measurement of the W^+ branching ratio into $u\bar{d}$ and $c\bar{s}$. The elements of the Cabibbo-Kobayashi-Maskawa (CKM) matrix, V^{CKM}, connecting the mass eigenstates with the weak eigenstates in the Standard Model of electroweak interactions, are known with poor precision for the second generation. Hadronic decays of the W boson allow a measurement, as the branching fractions are proportional to the appropriate squared modulus of the element of the CKM matrix. The strangeness content of the W^+ decay into $c\bar{s}$ allows the separation from the $u\bar{d}$ decay

Decays of W bosons, produced at LEP 200, can be exploited to measure the $\left|V_{cs}^{CKM}\right|$ element of the Cabibbo-Kobayashi-Maskawa matrix. The value can be extracted either from the measured hadronic branching ratio of W decays or by tagging the flavour of hadronic jets produced in W decays. Applying the two methods on the data collected during the first year of the LEP high-energy run, DELPHI obtains[31]

$$\left|V_{cs}^{CKM}\right| = 0.91\ ^{+0.15}_{-0.14}\ (\text{stat})\ ^{+0.05}_{-0.04}\ (\text{syst}).$$

The decay of W^+ into $c\bar{s}$ produced high momentum kaons, either from the primary strange quark or from decay of the charm quark.

7 Conclusions

The operation of a RICH detector is a very difficult and heavy task requiring a lot of efforts by many people. The operation of the DELPHI RICH has now become very stable after many years of efforts and learning. The impact of a RICH detector in physics analysis is significant because in some cases RICHes give the capability to obtain unique results while in most cases results competitive with other techniques are obtained.

8 Acknowledgments

The author wishes to thank all people who contributed to design, build and operate the DELPHI RICH detector and those who contributed to the physics analysis. A special thank to E. Schyns, N. Neufeld, G. Piana, Olav Ullaland and Valerio Gracco.

References

[1] DELPHI Collaboration, Nucl. Instr. and Meth. A378 (1996) 57;
DELPHI Collaboration, Nucl. Instr. and Meth. A303 (1991) 233.

[2] E. G. Anassontzis et al., Nucl. Instr. and Meth. A323 (1992) 351;
W. Adam et al., Nucl. Instr. and Meth. A338 (1994) 284;
W. Adam et al., Nucl. Instr. and Meth. A343 (1994) 68;
W. Adam et al., Nucl. Instr. and Meth. A371 (1996) 12;
W. Adam et al., Nucl. Instr. and Meth. A360 (1995) 416.

[3] J. D. Jackson, *Classical electrodynamics*, New York, J. Wiley & Sons, 1967.

[4] C. Bourdarios et al., *A mesurement of inclusive kaon and proton production in* Z^0 *decays*, DELPHI Internal note 92-128 PHYS 227, 15 September 1992.

[5] D. F. Anderson, Nucl. Instr. and Meth. 178 (1980) 125;
R. Apsimon et al., Nucl. Instr. and Meth. A241 (1985) 339;
R. A. Holroyd et al., Nucl. Instr. and Meth. A261 (1987) 440;
R. A. Holroyd et al., J. Phys. Chem. 89 (1985) 4244.

[6] Nucl. Instr. and Meth. A343 (1994).

[7] Nucl. Instr. and Meth. A371 (1996).

[8] DELPHI Collaboration, *Charged Kaon Production in Tau Decays at LEP*, Phys. Lett. B334 (1994) 435;
E. Agasi, W. Hao, K. Osterberg and A. Petrolini, *Charged kaon identification with the RICH in* τ *decays*, Nucl. Instr. and Meth. A371 (1996) 215.

[9] A. Petrolini, *Studio della produzione di mesoni strani nei decadimenti del leptone* τ *con il rivelatore RICH dell'esperimento DELPHI a LEP*, PhD thesis, University of Genova, Italy, February 1995.

[10] G. Piana, *Studio di decadimenti rari del leptone* τ *utilizzando il rivelatore RICH dell'esperimento DELPHI al LEP*, PhD thesis, University of Genova, Italy, February 1997;
G. Piana, Preliminary results presented at the 1997 Joint APS/APPT Meeting, April 1997, Washinton, DC, USA.

[11] P. M. Kluit, *Physics with Ring Imaging Cherenkov detectors*, Nucl. Instr. and Meth. A371 (1996) 223.

[12] Phys. Lett. B379 (1996) 330.

[13] DELPHI Collaboration, *First Measurement of the Strange Quark Asymmetry at the* Z^0 *Peak*, Z. Phys. C67 (1995) 1;
O. Botner et al., Nucl. Instr. and Meth. A371 (1996) 204;
F. Cossuti et al.,Nucl. Instr. and Meth. A371 (1996) 219;
E. Boudinov et al., *Measurement of the strange quark forward-backward asymmetry at the* Z^0 *peak*, Presented at the International Europhysics Conference on High-Energy Physics (HEP 97), Jerusalem, 19-26 August 1997.

[14] The OPAL Collaboration, *Measurement of the Branching Fractions and Forward-Backward Asymmetries of the* Z^0 *into Light Quarks*, Zeit. fur Physik C76 (1997) 387-400.

[15] SLD Collaboration, Preliminary results presented at the 1998 Joint APS/APPT Meeting, April 1998, Columbus, OH, USA.

[16] T. Sjöstrand, Comp. Phys. Comm. 39 (1986) 347;
T. Sjöstrand, M. Bengtsson, Comp. Phys. Comm. 43 (1987) 367;
T. Sjöstrand, Comp. Phys. Comm. 82 (1994) 74.

[17] G. Marchesini and B. Webber, Nucl. Phys. B238 (1984) 1;
G. Marchesini et al., Comp. Phys. Comm. 67 (1992) 465;
G. Marchesini et al., HERWIG 5.8c manual.

[18] Int. J. Mod. Phys. A12 2429.

[19] DELPHI Collaboration, *Inclusive Measurements of the* $K^{\pm}$ *and* $p\bar{p}$ *Production in Hadronic* Z^0 *Decays*, Nucl. Phys. B444 (1995) 3;
E. Schyns, PhD Thesis, WUB-DIS 96-22, University of Wuppertal, Germany;
DELPHI Collaboration, paper to be submitted.

[20] E. Schyns, *Pions, kaons and protons tagging for DELPHI RICHes*, DELPHI Internal note 96-103 RICH 89, 1 July 1996.

[21] DELPHI Collaboration, P. Abreu et al., Z. Phys. C73 (1996) 11.

[22] Particle Data Group, R. Barnett et al., Phys. Rev. D54, (1996) 1.

[23] OPAL Collaboration, R. Akers et al., Z. Phys. C63 (1994) 181-195.

[24] DELPHI Collaboration, P. Abreu et al., Phys. Lett. B444(1995) 3.

[25] DELPHI Collaboration, P. Abreu et al., Phys. Lett. B347(1995) 447-466.

[26] DELPHI Collaboration, P. Abreu et al., CERN–PPE/97-108, Measurement of the Quark and Gluon Fragmentation Functions in Z Hadronic Decays.
Accepted by E. Phys. J. C.

[27] OPAL Collaboration, R. Akers et al., Phys. Lett. B352 (1995) 176-186.

[28] SLD Collaboration, K. Abe et al., SLAC-PUB-96-7172.

[29] DELPHI Collaboration, preliminary results presented at the early 1998 conferences;
N. Neufeld, *Identified particles at LEP II* Lake Luise Winter Institute 1998.

[30] DELPHI Collaboration, *Search for Stable Heavy Charged Particles in* e^+e^- *Collisions at* $\sqrt{s} = 130 - 136, 161, 172$ GeV, Phys. Lett. B396 (1997) 315.

[31] B. Erzen, Preliminary results presented at the 1998 Joint APS/APPT Meeting, April 1998, Columbus, OH, USA.